

## STUDY OF THE U AND Th SERIES IN *Crassostrea mangle* SHELL

Wellington M. Farias<sup>1</sup>, Sandra R. Damatto, Luiz R. L. Simone, Vanessa S. Amaral,  
Paulo S. C. Silva<sup>1</sup>

<sup>1</sup> Instituto de Pesquisas Energéticas e Nucleares (IPEN / CNEN - SP)  
Av. Professor Lineu Prestes 2242  
05508-000 São Paulo, SP  
[wellington.m@usp.br](mailto:wellington.m@usp.br)  
[damatto@ipen.br](mailto:damatto@ipen.br)  
[pscsilva@ipen.br](mailto:pscsilva@ipen.br)

<sup>2</sup> Museu de Zoologia da USP (Mzusp)  
Avenida Nazaré, 481 - Ipiranga, São Paulo – SP  
04263-000 São Paulo, SP  
[lrsimone@usp.br](mailto:lrsimone@usp.br)  
[vanessamolusco@gmail.com](mailto:vanessamolusco@gmail.com)

### ABSTRACT

Foraminifera, corals and mollusks shells have been used as proxies for environmental, paleoenvironmental and climatic change studies in marine system by using elemental and isotopic ratios as recorder of such events. Nevertheless, there is little information available on the U and Th radionuclides decay series applied on those fields. In this sense, the objective of this paper was to evaluate the activity concentrations of the U and Th nuclide decay series in *Crassostrea mangle* shell samples as a function of the geographic location. Samples from São Paulo, Paraná, Alagoas, Rio Grande do Norte and Pernambuco states were analyzed by Neutron Activation Analysis and Gross Alpha and Beta Counting. Statistical analysis applied to the obtained results allowed differencing samples coming from São Paulo from that coming from Paraná.

### 1. INTRODUCTION

Several indicators have been employed as paleoenvironmental proxy, such as isotope ratio analysis of C, O, N and S stable isotopes, pollen and phytolith in soil core samples [1-6], sponge spicules, diatoms and foraminifera in sediment cores [7-13], tree growth ring in dendrochronology [14-15], coral and limestone shells of mollusks [16-18], among others.

In paleoenvironmental studies, sclerochronology, the physical and chemical changes in the growth of rigid structures study in the context of their formation may allow for environmental reconstruction based on the study of the chemical composition of clam shells, since these organisms build their carbonate parts from ions present in their environment [19]. Mollusk shells grow in the benthic region of coastal areas and they are of particular interest since their calcareous shells are influenced by environmental conditions of the surrounding water.

Foraminifera, corals and mollusks shells have been used as proxies for environmental, paleoenvironmental and climatic change studies in marine system by using elemental and isotopic ratios as recorder of such events. Nevertheless, there is little information available on the U and Th radionuclides decay series applied on those fields. In this sense, the objective of this work was to evaluate the activity concentrations of the U and Th nuclide decay series as

a function of the geographic location of sample collection and verify if their activity concentrations can be used as a proxy for environmental changes.

## 2. METHODOLOGY

### 2.1 Sampling

The shell samples from São Paulo state were obtained from a breeding oyster farm located in the Cananéia City. The samples from the states of Rio Grande do Norte, Pernambuco, Paraná and Alagoas were obtained from the Zoology Museum of São Paulo University, were all the samples were identified as *Crassostrea mangle* species.

### 2.2 Samples Preparation

All the samples were thoroughly washed with tap water, dried at 60°C in an oven and the outer layer was mechanically removed until just the carbonate matrix was left. The samples were immersed in a 4% hydrochloride acid for about 2 minutes and once more thoroughly washed with ultrapure water, dried and sieved to a grain size of 0.150 mm.

### 2.3 Instrumental Neutron Activation Analysis - INAA

Approximately 100 mg of powdered samples were precisely weighted in polyethylene bags and the irradiation time was set at 7 hours. The irradiation was performed at the IEA-R1 nuclear reactor under a neutron flux of  $10^{12}$  n cm<sup>-2</sup> s<sup>-1</sup>. The decay time lasted 7 days for U measurement and 14 days to Th measurement and the counting time was set at 2 hours. Certified reference material Estuarine Sediment, SRM 1646a (ES) from National Institute of Standards and Technology (NIST), Syenite, Table Mountain (STM) from United States Geological Survey (USGS) and the standard solutions (SPEX Certiprep) pipetted on filter paper were irradiated together with samples under the same conditions.

The gamma transition radiation measurement was performed by using an high pure germanium detector EG & G ORTEC model GEM with 20% of efficiency and nominal resolution of 1.9 keV for the 1332 keV gamma ray of <sup>60</sup>Co.

The concentrations were obtained comparing the photopeak area of the interest element in the sample spectrum with the photopeak area of the reference material, using the following expression (1):

$$C_{ai} = \frac{(A_{ai} m_p C_{pi}) e^{\lambda(t_a - t_p)}}{A_{pi} m_a} \quad (1)$$

Where:

- $C_{ai}$  is the elemental concentration in the sample (in  $\mu\text{g g}^{-1}$ );
- $C_{pi}$  is the elemental concentration in the standard (in  $\mu\text{g g}^{-1}$ );
- $A_{ai}$  is the activity from  $i$  element in the sample (in count per second);
- $A_{pi}$  is the activity from  $i$  element in the standard (in count per second);
- $w_a$  and  $w_p$  are the weights of the sample and standard (g), respectively;
- $\lambda$  is the decay constant of the  $i$  element and;
- $(t_a - t_p)$  difference of time between sample and standard counting.

## 2.4 Determination of $^{228}\text{Ra}$ , $^{226}\text{Ra}$ , and $^{210}\text{Pb}$

Approximately 1.00 g of the sample, in duplicate, were dissolved in mineral acids in hot plate with concentrated  $\text{HNO}_3$  and submitted to a radiochemical procedure for the determination of  $^{226}\text{Ra}$ ,  $^{228}\text{Ra}$  and  $^{210}\text{Pb}$ . An initial precipitation of Ra and Pb with  $3 \text{ mol L}^{-1} \text{ H}_2\text{SO}_4$ , is followed by dissolution with nitrile-tri-acetic acid at basic pH, precipitation of  $\text{Ba(Ra)SO}_4$  occurs with ammonium sulfate and precipitation of  $\text{PbCrO}_4$ , with 30% sodium chromate [20].

The  $^{226}\text{Ra}$  and  $^{228}\text{Ra}$  concentration were determined by gross alpha and beta counting of the precipitate of  $\text{Ba(Ra)SO}_4$  and the  $^{210}\text{Pb}$  concentration through its decay product  $^{210}\text{Bi}$ , by measuring the gross beta activity of the precipitate  $\text{PbCrO}_4$ . All the radionuclides were measured in a low background gas flow proportional detector for 200 minutes.

## 3. RESULTS AND DISCUSSION

Uranium and thorium concentrations were below the detection limits (DT) in all the analyzed samples. The typical DT for the neutron activation analysis in the same conditions that these samples were analyzed are  $0.1 \mu\text{g g}^{-1}$  for U and  $0.06 \mu\text{g g}^{-1}$  for Th. Although varying according to the species and geographical location the U concentrations in bivalves were reported in the range of  $0.04$  to  $0.3 \mu\text{g g}^{-1}$  [21] and from  $0.02$  to  $0.09 \mu\text{g g}^{-1}$  [22].

The carbonate phase of the mollusk shell generally contain insignificant amount of  $^{232}\text{Th}$ , reflecting the very low thorium content in the seawater from which it grew. The  $^{232}\text{Th}$  measured in marine biogenic carbonate is generally attributed to detrital contamination that may contain significant amount of this nuclide [23].

Table 1 shows the activity concentrations of  $^{226}\text{Ra}$ ,  $^{228}\text{Ra}$ , and  $^{210}\text{Pb}$  measured in the samples. The activity concentration of  $^{226}\text{Ra}$  varies from  $5.6$  to  $11 \text{ Bq kg}^{-1}$ , with a mean value of  $8.2 \pm 2 \text{ Bq kg}^{-1}$ ;  $^{228}\text{Ra}$  varies from  $134$  to  $187 \text{ Bq kg}^{-1}$ , with a mean value of  $156 \pm 15 \text{ Bq kg}^{-1}$  and the activity concentration of  $^{210}\text{Pb}$  varies from  $7.5$  to  $25 \text{ Bq kg}^{-1}$ , with a mean value of  $16.5 \pm 5 \text{ Bq kg}^{-1}$ .

It also can be verified in Table 1 that  $^{210}\text{Pb}$  are in excess related to  $^{226}\text{Ra}$  in all the samples. The radionuclide  $^{210}\text{Pb}$  is highly particle reactive and its residence time is very short in the coastal waters [24]. This excess may be related to the unsupported  $^{210}\text{Pb}$  due to the atmospheric  $^{222}\text{Rn}$  decay.

Radium-228 is 15 to 25 times higher than  $^{226}\text{Ra}$  in these samples. This enrichment has already been reported for calcified structures, such as mollusk shells [25], suggesting that the  $^{228}\text{Ra}$  in such structures may be due to uptake of  $^{232}\text{Th}$ . Nevertheless, the  $^{232}\text{Th}$  activities in the present samples were below the detection limit indicating, that the environment where the *C. mangle* grew up was possible rich in particulate matter containing high  $^{232}\text{Th}$  amount. These features fit into a marine environment that receives great influence of river discharges.

Divalent cations (mainly alkaline earths) such as Sr, Ba, and Ra are incorporated into the carbonate matrix by isomorphic substitution [26]. As it can be observed in Fig. 1 it looks to be the case of the  $^{226}\text{Ra}$  and  $^{228}\text{Ra}$  incorporation. The good agreement in the correlation coefficient indicates that these radionuclides are taken by the same processes. On the other hand, a different process must govern the *Crassostrea mangle*  $^{210}\text{Pb}$  uptake.

**Table 1: Activity concentration of the determined radionuclides in Bq kg<sup>-1</sup>, <sup>210</sup>Pb/<sup>226</sup>Ra, and <sup>228</sup>Ra/<sup>226</sup>Ra**

Sample	<sup>226</sup> Ra	<sup>210</sup> Pb	<sup>228</sup> Ra	<sup>210</sup> Pb/ <sup>226</sup> Ra	<sup>228</sup> Ra/ <sup>226</sup> Ra
RN 01	8.3 ± 2.9	14 ± 2	175 ± 4	2.3	20
AL 01	7.0 ± 0.2	16 ± 1	163 ± 1	2.3	23
AL 02	11 ± 1	18 ± 2	160 ± 9	1.6	15
PE 01	6.0 ± 1.6	16 ± 2	145 ± 10	3.2	19
SP 01	5.6 ± 0.5	8.7 ± 0.8	141 ± 3	3.4	22
SP 02	7.6 ± 0.1	17 ± 1	153 ± 15	1.0	17
SP 03	7.5 ± 0.3	24 ± 1	141 ± 7	1.9	16
SP 04	7.2 ± 0.4	25 ± 3	160 ± 3	1.3	17
SP 05	7.7 ± 0.9	7.5 ± 1	134 ± 6	1.9	17
PR 01	11 ± 2	21 ± 2	187 ± 8	1.7	21
PR 02	9.0 ± 0.6	11 ± 1	157 ± 2	2.7	24
PR 03	9.7 ± 0.4	18 ± 2	165 ± 2	1.6	25

Cluster analysis applied to the samples, showed in Fig. 2, resulted in two groups. A good differentiation can be seen between the São Paulo and Paraná samples. Nevertheless, the northeast samples did not present a clear pattern, possibly because of the lower number of samples.

#### 4. CONCLUSIONS

Samples of *C. mangle* shell from different regions were analyzed by INAA and total alpha and beta counting. The results showed that the samples present low U and Th concentrations, below the detection limit, and low content of <sup>226</sup>Ra. The observed excess of <sup>210</sup>Pb must be related to the enrichment of this nuclide in the coastal water where these mollusks grow due to <sup>222</sup>Rn decay, as well as, the enrichment in <sup>228</sup>Ra must be related to the <sup>232</sup>Th adsorbed in the suspended particulate matter. Statistical analysis just permitted differentiates samples coming from São Paulo of that coming from Paraná. The results indicate that with further analysis of a higher number of samples from the studied regions will possibly allow determining their provenance with a better precision.

Paraná and São Paulo samples are characterized by higher <sup>226</sup>Ra content and lower <sup>210</sup>Pb/<sup>226</sup>Ra and <sup>228</sup>Ra/<sup>226</sup>Ra ratios.

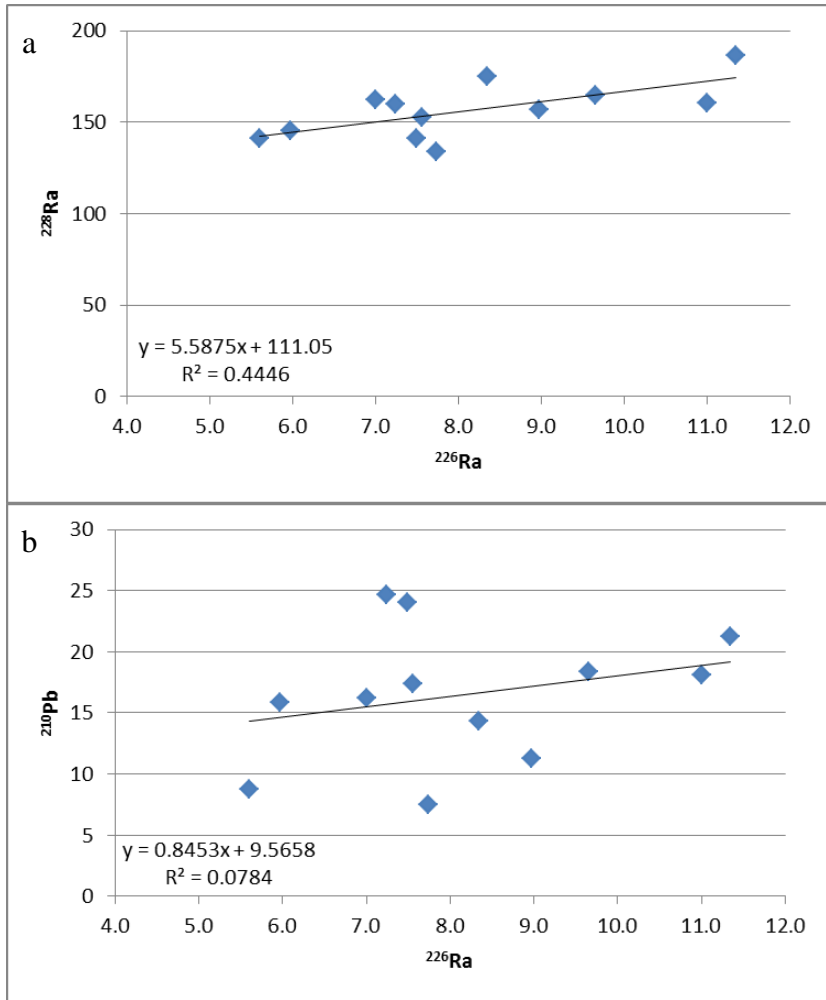


**Figure 1: Correlation coefficient a)  $^{226}\text{Ra}$  and  $^{228}\text{Ra}$  and b)  $^{226}\text{Ra}$  and  $^{210}\text{Pb}$ .**

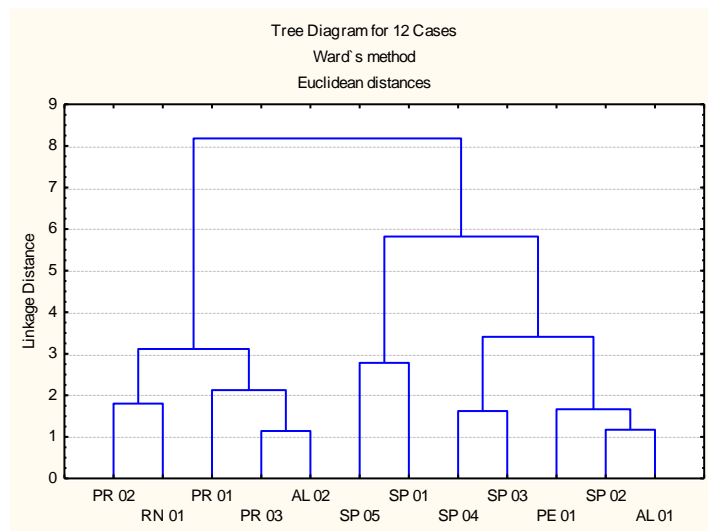


**Figure 2: Cluster analysis applied to the samples.**

## REFERENCES

1. Kellya, E. F., Bleckera, S.W., Yonkera, C. M., Olsonb, C. G., Wohlc, E. E., Todd, L. C., 1998. Stable isotope composition of soil organic matter and phytoliths as paleoenvironmental indicators, *Geoderma*, **82(1-3)**:59 -81.
2. Xiao, X., Shen, J., Wang, S., Xiao, H., Tong, G., 2008. The plant diversity and its relationship with paleoenvironment since 2.78 Ma revealed by pollen records in the Heqing deep drilling core, *Chinese Science Bulletin*, **53(23)**: 3686-3698.
3. Alexandre, A., Crespin, J., Sylvestre, F., Sonzogni, C., Hilbert, D. W., 2012. The oxygen isotopic composition of phytolith assemblages from tropical rainforest soil tops (Queensland, Australia): validation of a new paleoenvironmental tool, *Clim. Past*, **8**: 307–324.
4. Leybourne, M. I., Cameron, E. M., Reich, M., Palacios, C., Faure, K., Vincent, M., Rafélis, M., Lartaud, F., Fialin, M., Verrecchia, E., 2013. Chemical labelling of oyster shells used for time-calibrated high-resolution Mg/Ca ratios: a tool for estimation of past seasonal temperature variations, *Palaeogeography, Palaeoclimatology, Palaeoecology*, **373**: 66-74.
5. Ryota, O., Tatsuichiro, K., Jun, I., 2012. Holocene history of intentional fires and grassland development on the Soni Plateau, Central Japan, reconstructed from phytolith and macroscopic charcoal records within cumulative soils, combined with paleoenvironmental data from mire sediments, *Holocene*, **22(7)**: 793-800.
6. Zheng, Z., Huang K. Y., Deng Y., Cao L. L., Yu S. H., Suc, Jp., Berne, S., Guichard, F., 2013. A ~200 ka pollen record from Okinawa Trough: Paleoenvironment reconstruction of glacial-interglacial cycles, *Sci China Earth Sci*. **56(10)**: 1731-1747.
7. Trombold, C. D., Israde-Alcantara, I., 2005. Paleoenvironment and plant cultivation on terraces at La Quemada, Zacatecas, Mexico: the pollen, phytolith and diatom evidence, *Journal of Archaeological Science*, **32(3)**: 341–353.
8. Barth, O. M.; Sao-Thiago, L. E. U; Barros, M. A., 2006. Paleoenvironment interpretation of a 1760 years BP old sediment in a mangrove area of the Bay of Guanabara, using pollen analysis, *Anais da Academia Brasileira de Ciências*, **78(2)**: 227-229.
9. Wirrmanna, D., Sémahb, A., Chacornac-Raultb, M., 2006. Late Holocene paleoenvironment in northern New Caledonia, southwestern Pacific, from a multiproxy analysis of lake sediments, *Quaternary Research*, **66(2)**: 213–232.
10. Volkmer-Ribeiro, C., Ezcurra de Drago, I., Parolin, M., 2007. Spicules of the Freshwater Sponge Ephydatia facunda Indicate Lagoonal Paleoenvironment at the Pampas of Buenos Aires Province, Argentina, *Journal of Coastal research*, **50**: 449-452.
11. Fukumoto, Y., 2011. Mid-late Holocene paleoenvironment in Karako lowland, western Japan, inferred from diatom analysis, *Quaternary International*, **230(1-2)**: 115-121.
12. Wang, Y., Liu, X., Mischke, S., Herzsuh, U., 2012. Environmental constraints on lake sediment mineral compositions from the Tibetan Plateau and implications for paleoenvironment reconstruction, *Journal of Paleolimnology*, **47(1)**: 71-85.

13. Dubicka, Z., Peryt, D., Szuszkiewicz, M., 2014. Foraminiferal evidence for paleogeographic and paleoenvironmental changes across the Coniacian–Santonian boundary in western Ukraine, *Palaeogeography, Palaeoclimatology, Palaeoecology*, **401(1)**: 43–56.
14. Strachan, S., Biondi, F., Lindstroem, S., McQueen, R., Wigand, P., 2013. Application of Dendrochronology to Historical Charcoal-Production Sites in the Great Basin, United States, *Historical Archaeology*, **47(4)**: 103-119
15. Gebrekirstos, A., Bräuning, A., Sass-Klassen, U., Mbow, C., 2014. Opportunities and applications of dendrochronology in Africa, *Current Opinion in Environmental Sustainability*, **6**: 48–53.
16. Schöne, B. R., 2013. *Arctica islandica* (Bivalvia): A unique paleoenvironmental archive of the northern North Atlantic Ocean, *Global and Planetary Change*, **111**: 199–225.
17. Sessa, J. A., Callapez, P. M., Dinis, P. A., Hendy, A. J. W., 2013. Paleoenvironmental and Paleobiogeographical Implications of a Middle Pleistocene Mollusc Assemblage from the Marine Terraces of Baía Das Pipas, Southwest Angola, *Journal of Paleontology*, **87(6)**:1016-1040
18. Faranda, C., Gliozzi, E., Cipollari, P., Grossi, F., Darbaş, G., 2013. Messinian paleoenvironmental changes in the easternmost Mediterranean Basin: Adana, Basin, southern Turkey, Turkish, *J Earth Sci*, **22**: 839-863.
19. Mouchi, V., Rafélis, M., Lartaud, F., Fialin, M., Verrecchia, E., 2013. Chemical labelling of oyster shells used for time-calibrated high-resolution Mg/Ca ratios: A tool for estimation of past seasonal temperature variations, *Palaeogeography, Palaeoclimatology, Palaeoecology*, **373 (1)**: 66–74.
20. Leonardo, L., Damatto, S. R., Gios, B. R., Mazzilli, B. P. 2014. Lichen specie *Canoparmelia texana* as bioindicator of environmental impact from the phosphate fertilizer industry of São Paulo, Brazil, *Journal of Radioanalytical and Nuclear Chemistry*, **299 (3)**: 1935-1941.
21. Kaufman, A., Ghaleb, B., Wehmiller, J. F., Hillarie-Marcel, C., 1996. Uranium concentration and isotope ratio profiles within *Mercenarius* shells: Geochronological implications, *Geochimica et Cosmochimica Acta*, **60 (19)**: 3735-3746.
22. Choukri, A., Hakam, O.-K., Reyss, J.-L., Plaziat, J.-C., 2007. Radiochemical dates obtained by alpha spectrometry on fossil mollusk shell from the 5e Atlantic shoreline of the High Atlas, Morocco, *Applied Radiation and Isotopes*, **65 (8)**: 883-890.
23. Staubwasser, M., Henderson, G. M., Berkman, P. A., Hall, B. L., 2004. Ba, Ra, Th, and U in marine mollusc shells and the potential of <sup>226</sup>Ra/Ba dating of Holocene marine carbonate shells, *Geochimica et Cosmochimica Acta*, **68 (1)**: 89-100.
24. Baskaran, M., Santschi, P.H., 1993. The role of particles and colloids in the transport of radionuclides in coastal environments of Texas, *Mar. Chem*, **43**: 95–114.

25. IAEA, International Atomic Energy Agency. *The Environmental Behaviour of Radium: Revised Edition*. TECHNICAL REPORTS Series No. 476, 2014.
26. Baskaran, M., Hong, G., Kim, S., Wardle, W. J., 2008. Reconstructing seawater column  $^{90}\text{Sr}$  based upon  $^{210}\text{Pb}/^{226}\text{Ra}$  disequilibrium dating of mollusk shells, *Applied Geochemistry*, **20**: 1965–1973.